

**Interfacial magnetic structure in Fe/NiO(001)**P. Luches,<sup>1</sup> L. Pasquini,<sup>2</sup> S. Benedetti,<sup>1</sup> V. Bellini,<sup>1,3</sup> S. Valeri,<sup>1,3</sup> F. Manghi,<sup>1,3</sup> R. Rüffer,<sup>4</sup> and F. Boscherini<sup>2</sup><sup>1</sup>*S3, Istituto Nanoscienze - CNR, Via G. Campi 213/a, I-41125 Modena, Italy*<sup>2</sup>*Physics Department and CNISM, University of Bologna, Viale C. Berti-Pichat 6/2, I-40127 Bologna, Italy*<sup>3</sup>*Physics Department, University of Modena, Via G. Campi 213/a, I-41125 Modena, Italy*<sup>4</sup>*European Synchrotron Radiation Facility, BP 220, F-38043, Grenoble Cedex, France*

(Received 19 October 2010; revised manuscript received 14 January 2011; published 15 March 2011)

Using nuclear resonant scattering of synchrotron radiation and density functional theory calculations we have resolved the magnetic properties of the different Fe phases present at the Fe/NiO(001) interface, an epitaxial ferromagnetic/antiferromagnetic system. We have detected the presence of an interfacial antiferromagnetic FeO-like phase with a significantly increased magnetic moment compared to the case of a sharp interface. Already a few atomic layers above the interface, the Fe atoms have a bulk-like metallic character and the reversal of their magnetization is strongly influenced by the antiferromagnetic layer.

DOI: [10.1103/PhysRevB.83.094413](https://doi.org/10.1103/PhysRevB.83.094413)

PACS number(s): 75.70.-i, 76.80.+y

**I. INTRODUCTION**

Nanocomposite magnetic systems composed of different phases, each exhibiting a specific magnetic behavior and coupled by their mutual interaction, can be designed to obtain artificial materials with novel and potentially useful magnetic properties. Among these systems of particular interest are coupled ferromagnetic (FM)/antiferromagnetic (AFM) materials, which present a unidirectional anisotropy, known as exchange bias.<sup>1,2</sup> An insightful understanding and control of the magnetic properties of nanocomposite systems requires a description of the materials at the atomic scale. A general quantitative explanation of the exchange bias is still not available, in spite of the great effort by many researchers and the numerous studies performed; there is a consensus that this is mostly due to a poor understanding of the interface between the two materials in terms of its local atomic structure and magnetic couplings. In general, the magnetic structure of FM/AFM interfaces has to be taken into consideration in the models to correctly predict the overall magnetic behavior of the investigated system.

To simplify at least part of the complexity of these systems, well-controlled epitaxial FM/AFM bilayers can be used in experimental studies. Oxides have been very often used as AFM materials due to their relatively high Néel temperature, good chemical and mechanical stability, and wide band gap.<sup>3</sup> NiO and CoO are the most frequently used oxide AFM layers in these studies<sup>3-12</sup> and Fe grows epitaxially on both of them. Unlike CoO, NiO has a Néel temperature significantly larger than room temperature (RT) and it is therefore suitable to be used in applications. On the other hand, however, CoO shows a lower tendency to be reduced than NiO. Fe/NiO(001) bilayers present a good epitaxial quality, a relatively large value of exchange bias, and no training effect. In this system the epitaxial interface has been characterized in great detail in its composition and structure, finding that Fe is partly oxidized<sup>6,7,9</sup> and forms an interfacial planar FeO-like layer, while a few NiO layers are reduced<sup>6,7,9</sup> and the metallic Ni atoms are incorporated into the first layers of the Fe film in a strained bcc phase.<sup>11</sup> *Ab initio* calculations of the structural and electronic properties of the same system have predicted that the Fe atoms in the FeO-like phase at the interface have an increased

magnetic moment compared to the sharp interface.<sup>10,13</sup> A correct experimental assessment of the magnetic properties of this low-dimensional interfacial phase is crucial due to its fundamental role in determining the interface magnetic couplings.

Probing the magnetic properties of a buried interfacial layer is a very challenging task. In particular, in the case of FM/AFM systems based on AFM oxide x-ray magnetic circular (XMCD) and linear (XMLD) dichroism techniques, due to their chemical sensitivity, can be used for this purpose, although in this case the depth sensitivity is indirectly inferred from the observation of chemical states different from the nominal one, which are ascribed to interfacial phases. A true depth resolution can be obtained by isotope-sensitive techniques, such as Mössbauer spectroscopy and nuclear resonance scattering (NRS) of synchrotron radiation, which exploit the variations of hyperfine splitting of nuclear levels to obtain information on the local magnetic properties.<sup>14</sup> The subnanometric depth resolution of these techniques is obtained by the use of an ultrathin <sup>57</sup>Fe probe layer placed at different distances from the interface during growth.

Using XMCD and XMLD in the Co/NiO system NiO has been found to be partially reduced by Co deposition forming a mixed Co- and Ni-oxide phase in which a fraction of Ni atoms were found to be FM, while no evidence for AFM alignment in oxidized Co was detected.<sup>4</sup> Using the same techniques in the Fe/CoO system the observed uncompensated FM spins at the CoO interface have been found to be mainly of oxide character and a FeO-like phase has been detected at the interface, similarly to the Fe/NiO case, although to a lower extent.<sup>5</sup> The magnetic properties of the FeO-like phase have not been investigated.

Depth-resolved magnetic studies of composite systems,<sup>15</sup> including FM/AFM bilayers,<sup>16-20</sup> have also been performed by isotope sensitive techniques. However, the magnetism of the real interface layers is very difficult to be investigated or determined due to their complicated hyperfine-field distribution induced by their structural and magnetic complexity.<sup>19</sup>

In this work we show that it is possible to resolve the magnetic complexity of the interface between Fe and NiO by combining the experimental NRS results with density-functional theory (DFT) calculation of nuclear hyperfine fields in the system. DFT has, in fact, shown to be of

invaluable help to assist the correct interpretation of nuclear probe experiments.<sup>21</sup> With this approach we characterize the magnetic properties of the different structural and chemical phases present at the Fe/NiO interface.

## II. EXPERIMENTAL AND THEORETICAL DETAILS

For the experimental part of this study we used two Fe/NiO bilayers grown on Ag(001) single crystals. The NiO films and the Fe layers were grown in an ultrahigh vacuum by molecular beam epitaxy, using the procedures described in our previous studies.<sup>7,10,11</sup> The epitaxial NiO films were 10-nm thick. An overall Fe layer thickness of 13 ML (1 Fe ML = 1.435 Å) was chosen for the two samples. This value is significantly greater than that necessary for the onset of ferromagnetism at RT.<sup>8</sup> Both samples contain a 2 ML <sup>57</sup>Fe (95.5% enriched) probe layer located at different distances from the interface with NiO: one sample contains the probe layer at the interface with NiO, while the other contains the probe layer 7 ML above the interface; the samples will be referred to as “interface” (IF) and “inside” (IN), respectively. The thickness of the probe layer has been chosen to be 2 ML, rather than 1 ML, to optimize count rate. Even at the interface this should not change the information because at the first stages of growth Fe forms islands 2–3-ML thick on NiO.<sup>8</sup> Both samples were capped by a 5-nm thick Ag layer to prevent oxidation of the Fe films, and they were kept in a nonreactive atmosphere during their transfer to the synchrotron radiation laboratory.

The NRS measurements were performed at the Nuclear Resonance (ID18) beamline<sup>22</sup> of the European Synchrotron Radiation Facility (ESRF) in Grenoble. The storage ring was operated in the 16-bunch mode, which guarantees a time interval between two subsequent pulses (176 ns) long enough to accurately measure the decay of the scattered radiation from nuclear excited states at the 14.4-keV resonance of <sup>57</sup>Fe (lifetime 141 ns). By analyzing the beat pattern originating from the simultaneous decay of energetically split nuclear energy levels we determined the hyperfine field, the isomer shift, and the projection of the magnetization vector along the direction of the photon wave vector of the different Fe phases in the investigated samples. The 14.4-keV photon beam was focused to  $15 \times 15 \mu\text{m}^2$  and the measurements were performed in grazing incidence geometry at the critical angle for total external reflection (4 mrad) to maximize the count rate. The measurements were performed at RT in an external magnetic field  $\vec{H}$  collinear to the Fe[100] in-plane direction and to the photon wave vector  $\vec{k}$ . All of the data shown in this study were acquired before any field cooling process of the system.

DFT calculations of the magnetic hyperfine field were performed by means of the WIEN2K code.<sup>23</sup> In Fig. 1 we illustrate the three systems considered. Slab-supercell calculations were used to study the Fe/NiO(001) interface in the presence of 0, 1, or 2 in-plane oxidized Fe layers at the interface with NiO; for computational reasons the total number of Fe layers was limited to five, and the Fe overlayer was placed at both sides of a five layer NiO slab substrate (enough to retain a bulk behavior in the inner NiO layer). In-plane and out-of-plane periodicity of the simulation cell were chosen as such to host the AFM magnetic ordering of the NiO substrate (we considered the NiO surface to attain the same magnetic ordering of NiO bulk,

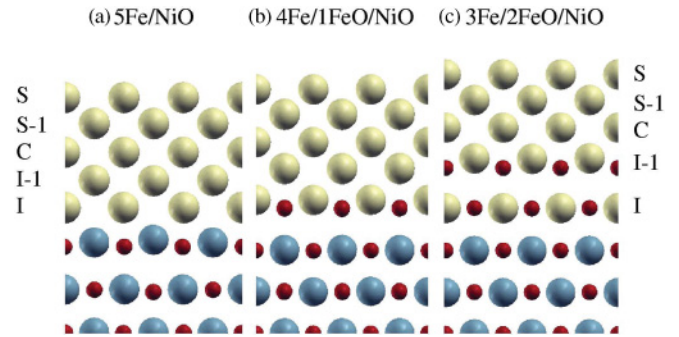


FIG. 1. (Color online) Sketches of the three model systems considered to simulate the Fe/NiO interface with (a) 0 FeO layers, (b) 1 FeO layer, and (c) 2 FeO layers. Small black circles (red): O, big gray circles (blue): Ni, and big, light gray circles (yellow): Fe.

named in the following AFM-AF2) and to isolate the slab replicas (more details can be found in Ref. 10 for the very same interface, but with a different number of Fe overlayers). AFM-AF2 ordering was assumed for the Fe moments in the FeO layers, matching the one of the NiO layer below it. The structures were fully relaxed until remanent forces were less than 2 mRy/a.u. The major contribution to the hyperfine field arises from the contact term given by the Breit formula (for scalar-relativistic electrons), and is proportional to the spin density averaged within a sphere of Thomson radius around the nucleus. Other contributions, such as intra-atomic orbital and dipolar terms, are generally small and, in our case, will be neglected. To verify this statement, we calculated the orbital and dipolar contributions to the hyperfine fields for one of the systems [Fig. 1(b): Fe/1 ML FeO/NiO] described in the next section, and we found that they amount to less than 0.5 T for each of the Fe atoms. Since an intrinsic error bar of  $\pm 0.5$  T is anyhow expected in the calculated hyperfine fields, such contributions will not be considered. For a more in depth description of the method used to obtain the hyperfine fields from DFT we refer to the work by Blügel *et al.*<sup>24</sup>

## III. RESULTS AND DISCUSSION

Figure 2 shows the NRS time spectra measured at selected values of the external magnetic field along the decreasing-field branch of the hysteresis loop in the  $\vec{H} // \vec{k}$  configuration for the IN and IF samples. The single-frequency beat pattern observed for both samples at large positive applied fields confirms the expected dominant alignment of the magnetization collinear to the direction of the applied field.<sup>25</sup> The faster damping of the scattered intensity of the IF sample is an indication of the presence of different components and/or hyperfine field distributions, expected on account of the structural and chemical complexity at the interface. The different phases for each sample have been resolved by a least-squares fitting of the spectrum acquired at saturation magnetization (i.e., at about  $H = 950$  mT) using the NRS software package.<sup>26</sup> The IN sample spectrum [Fig. 2(a)] was fitted by a single component with a hyperfine field  $B_{\text{HF}} = -33.2$  T and a very narrow distribution (see Table I). The  $B_{\text{HF}}$  value of this phase is in good agreement with the one of metallic Fe in the bcc phase at RT, proving that already a few monolayers above the NiO

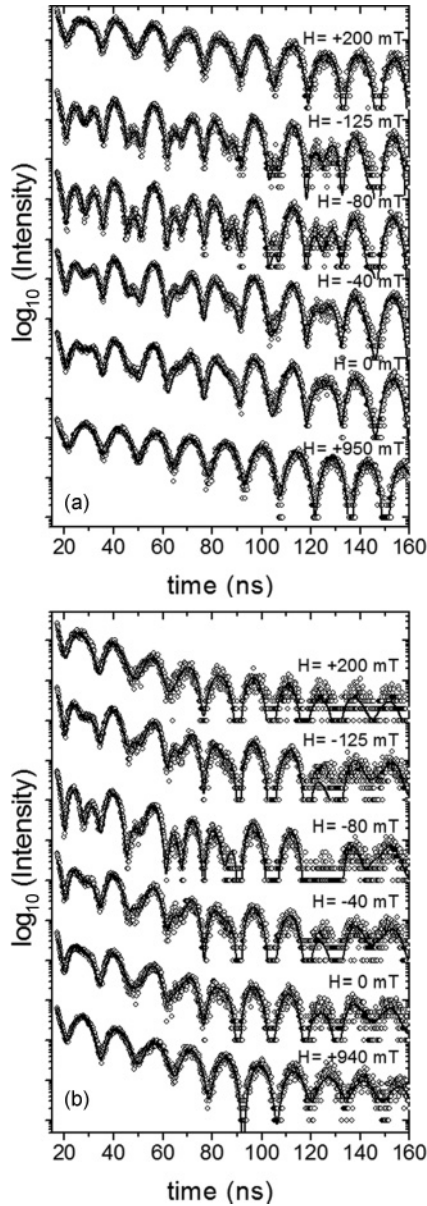


FIG. 2. NRS time spectra measured at selected values of the applied magnetic field  $H$  along the decreasing-field branch of the hysteresis loop for (a) the IN sample and (b) the IF sample at RT. The topmost spectrum is acquired at +200 mT along the increasing-field branch of the loop. The magnetic field  $H$  is applied collinear to the photon wave vector  $\vec{k}$ . The fits of the spectra are also reported as a solid line.

interface the Fe films have a bulk-like magnetic structure, confirming the limited extent of interfacial intermixing.<sup>11</sup> The fitting of the IF sample spectrum [Fig. 2(b)] was more complex and required three components, with the hyperfine parameters summarized in Table I. The first component, with the largest relative weight, has a  $B_{\text{HF}}$  value very close to the one of metallic bcc Fe. The other two components have a higher value of the isomer shift compared to the first one and a 20% relative weight each. They can be ascribed to Fe atoms with in-plane oxygen nearest neighbors, that is, atoms in the FeO-like phase at the interface, detected in our previous structural characterization of the Fe/NiO system.<sup>10</sup> The value measured for the isomer

TABLE I. Isomer shift (IS), hyperfine field ( $B_{\text{HF}}$ ), relative width of the hyperfine field distribution ( $\Delta B_{\text{HF}}/B_{\text{HF}}$ ), and relative weight (RW) of the different components used for the fitting of the NRS time spectra for the IN and IF samples in the  $\vec{H} \parallel \vec{k}$  configuration. Errors are indicated in parentheses.

Sample	Component #	IS (mm/s)	$B_{\text{HF}}$ (T)	$\Delta B_{\text{HF}} / B_{\text{HF}}$ (%)	RW (%)
IN	1	0 fixed	-33.2 (2)	2	100
IF	1	0 fixed	-33.5 (2)	6 (1)	60 (6)
	2	0.42 (5)	-37.2 (3)	11 (2)	20 (2)
	3	0.42 (5)	+25.3 (5)	90 (5)	20 (2)

shift of this component is intermediate between the one of bulk FeO (1 mm/s) and the metallic Fe one (0 mm/s).<sup>27</sup> It has to be noted that the overall relative weight of the two oxidized phases is slightly less than expected in the case of a complete FeO layer due to an island-like growth morphology at the early stages of interface formation.<sup>8</sup> The oxidized components have different values of  $B_{\text{HF}}$ . One of them has a negative  $B_{\text{HF}}$ , which is significantly greater in absolute value than the one of the metallic phases and close to the value measured at RT for FeO-like antiferromagnetic films,<sup>18</sup> The other one has a positive value of  $B_{\text{HF}}$  (i.e., it is oriented parallel to the applied magnetic field), smaller in magnitude with respect to the other ones, and a very broad distribution.

To understand the physical meaning of the oxidized components we compared the experimental hyperfine fields to the ones resulting from *ab initio* calculations for the three model structures shown in Fig. 1. Table II reports the values of the hyperfine fields for the two inequivalent Fe sites and of the magnetic moment (calculated integrating the spin charge inside muffin-tin spheres of 1.9 a.u. radius, centered at each atom) per Fe atom for each Fe atomic layer. For the model without the FeO layer the hyperfine fields at the layer close to NiO (I) are similar to the ones in the central layer (C) and both are close to the hyperfine field of ferromagnetic bcc bulk Fe;<sup>28</sup> only the Fe atom in the I-1 layer exhibits a more negative hyperfine field due to a reduction in the positive valence hyperfine field transferred by the magnetic environment. For the model with a single FeO layer we find that  $B_{\text{HF}}$  is more negative (-37 T) than in bulk Fe for one of the two inequivalent Fe sites, while the other one has a positive  $B_{\text{HF}}$  which is significantly smaller

TABLE II. Calculated hyperfine fields ( $B_{\text{HF}}$ ) and magnetic moments ( $m$ ) at the Fe layer of the three systems sketched in Fig. 1; two inequivalent atoms are present at each Fe layer, the latter being labeled as interface (I), above the interface (I-1), central (C), below the surface (S-1), and surface (S) layers.

System	5Fe/NiO		4Fe/1FeO/NiO		3Fe/2FeO/NiO	
	$B_{\text{HF}}$ (T)	$m$ ( $\mu\text{B}$ )	$B_{\text{HF}}$ (T)	$m$ ( $\mu\text{B}$ )	$B_{\text{HF}}$ (T)	$m$ ( $\mu\text{B}$ )
S	-25, -25	2.9	-24, -25	2.9	-22, -22	3.0
S-1	-37, -37	2.4	-37, -37	2.4	-37, -33	2.5
C	-32, -32	2.6	-32, -28	2.5	-25, -25	2.7
I-1	-38, -34	2.5	-31, -30	2.4	-37, +14	3.1
I	-32, -30	2.7	-37, +17	3.1	-35, +37	3.5

in absolute value than the first one; they are, respectively, associated to Fe atoms with up and down spin moments. Finally, for the model with two oxidized layers at the interface, there is a significant increase in the positive  $B_{\text{HF}}$  at the interface and the layer above (I-1) acquires an antiferromagnetic splitting. In simulations performed assuming a ferromagnetic coupling in the FeO layers (not shown), the oxidized Fe component shows neither a site with positive hyperfine fields nor one with a more negative hyperfine field (compared to bulk Fe), while it attains very similar values to the ones of metallic Fe.

The results of the theoretical model have been of great value to understand the magnetic properties of the interface. The experimental results, in particular, the experimentally measured broad  $B_{\text{HF}}$  distribution centered around positive values and the large negative value found in the fitting of the NRS spectra of the oxidized Fe components, are consistent with a situation which is a mixture of those sketched in Figs. 1(b) and 1(c) (i.e., where the first layer and part of the second layer are oxidized). The interesting result is not only the expected disagreement of the NRS data with the case of a sharp interface, but especially the fact that the data are consistent only with the hypothesis of an FeO layer (1–2-ML thick), which is antiferromagnetic and has an increased value of the Fe magnetic moment per atom compared to the case of the sharp interface. The unavoidable structural defects, the possible presence of a mixed Fe-Ni-O phase, and the non-perfectly flat morphology of the real interface result in a broad distribution of positive  $B_{\text{HF}}$  values rather than in two or three discrete values of  $B_{\text{HF}}$ . The presence of a dominant metallic phase at the interface demonstrates also that the interfacial reaction is limited to less than two layers and that the growth mode is island-like at least for low amounts of deposited Fe.

In the study of the Co/NiO system by Ohldag *et al.*<sup>4</sup> no linear magnetic dichroism was observed for the oxidized Co phase at variance with the results of this study on Fe/NiO, where a clear evidence for an AFM oxidized Fe phase is found. This is possibly due to the strong dependence of AFM anisotropy on the thickness and on the order of the observed intermixed phases formed at interface in the two systems.

The theoretical calculations also allow to understand the origin of the specific values of the hyperfine field in the FeO phase layer that is in contact with metallic Fe, that is, the negative  $B_{\text{HF}}$ , larger in absolute value than the positive  $B_{\text{HF}}$  value [I-layer in Fig. 1(b) and I-1 layer in Fig. 1(c)]. As is largely demonstrated, the hyperfine field of a specific atom in a solid is not simply proportional to its magnetic moment. Its value is given by the sum of two contributions. One of them originates from the polarization of the core electrons by the local  $d$  shell and it is proportional in magnitude, but opposed in sign to the magnetic moment of the atom. The other is a valence electron contribution, in turn, given by the sum of a local term, originating from the polarization of the local valence  $s$  electrons by the local  $d$  shell, and of a nonlocal term transferred by hybridization from the polarized  $d$  electrons of the surrounding atoms. The two inequivalent Fe sites within the interface FeO layer in Fig. 1(b) have the same magnetic moment (+3.1 and  $-3.1 \mu_{\text{B}}$ ), a similar value for the core contribution to the hyperfine field ( $-84$  and  $+81$  T, respectively) and a very different valence contribution

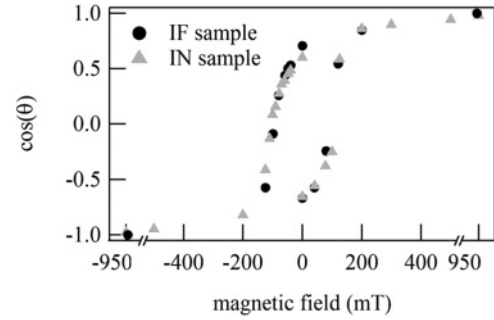


FIG. 3. Relative variation of the magnetization, obtained from the fitting of the NRS time spectra, along an external magnetic field cycle, for the metallic components used for the fitting of the NRS time spectra of the IN and IF samples (component #1 in Table I). The magnetic field  $H$  is applied collinear to the photon wave vector  $\vec{k}$  and to the Fe[100] orientation.

(+47 and  $-64$  T, respectively), which originates from the fact that the contributions transferred from the atoms in the above metallic layers are of opposite sign, reflecting the parallel/antiparallel alignment of the magnetic moments. The total transferred contribution of the other surrounding atoms is almost negligible since they are in an antiferromagnetic phase. The asymmetry in the value of the positive and negative hyperfine fields of the interface FeO phase originates therefore from the nonlocal contribution to  $B_{\text{HF}}$ . The same argument applies for the Fe atoms in contact with the metallic Fe phase in Fig. 1(c) (I-1 layer), while the Fe atoms of the I layer in the same figure are in a configuration much more similar to a bulk one and therefore the asymmetry in the positive and negative values of  $B_{\text{HF}}$  is almost completely removed.

The spectra of IN and IF samples [Figs. 2(a) and 2(b)] gradually evolve with decreasing applied magnetic field (from bottom to top). A nearly single-frequency beat pattern is recovered at fields more negative than  $-200$  mT and persists for increasing applied fields up to  $+200$  mT. From the spectra at different values of  $H$  it is possible to obtain the orientation of the magnetization of each component relative to the applied field. In the least-squares fitting of the spectra recorded for each value of  $H$ , the number of components and their hyperfine parameters were kept fixed, while the only free parameter for each component was an effective angle  $\theta$  whose cosine represents the projection of the component's magnetization  $\vec{M}$  along the direction of the photon wave vector  $\vec{k}$

$$\cos(\theta) = \frac{\vec{M} \cdot \vec{k}}{M^S k},$$

where  $M^S$  is the component's saturation magnetization.<sup>20,25</sup> Figure 3 shows the hysteresis loops obtained by reporting the variation of  $\cos(\theta)$  for the metallic phase for the two samples along a cycle of  $H$  from 1 to  $-1$  T and back. The metallic phase in the IF sample is due to an island growth mode of Fe at the first stages of growth.<sup>8</sup> The hysteresis loops of the metallic components for the two samples have the same shape, showing that the main mechanism for magnetization reversal is the same at the two distances from the interface. The loops show a very large coercive field (100 mT) compared not only to bulk Fe, but also to Fe films with similar thickness, structure, and

morphology, grown on a nonmagnetic oxide such as MgO.<sup>29</sup> This change in the magnetic properties of Fe is probably due to the strong coupling with the underlying antiferromagnetic NiO, which extends over several monolayers above the interface, mediated by the FeO-like antiferromagnetic phase at the interface. For the interfacial oxide phase, instead, the evolution of the spectra with the applied field reflects the changes in the hyperfine fields induced by the magnetization reversal of the ferromagnetic Fe phase. In general, the magnetic properties of the interfacial phases in FM/AFM systems are expected to have an influence on the exchange bias mechanism and they have to be taken into consideration in the models that try to explain the values of exchange bias field observed experimentally.

#### IV. CONCLUSION

In conclusion, by using NRS in grazing incidence with a probe layer approach and *ab initio* calculation of hyperfine

fields we have resolved the magnetic structure at and near the Fe/NiO(001) interface, a well-characterized ferromagnetic/antiferromagnetic coupled system. We obtained direct evidence for the presence of an antiferromagnetic FeO-like phase, confined over one or two layers at the interface, with a significantly increased magnetic moment compared to the case of a sharp interface. The layers inside, although metallic with bulk-like hyperfine parameters, are strongly coupled to the antiferromagnetic phase. As a consequence, the magnetization reversal of the metallic component at the interface and inside the film is very similar.

#### ACKNOWLEDGMENT

We acknowledge the European Synchrotron Radiation Facility for the provision of beamtime and logistic support for the experiment. This work was partially supported by MIUR through PRIN Project 20087NX9Y7.

- 
- <sup>1</sup>J. Nogués and I. K. Schuller, *J. Magn. Magn. Mater.* **192**, 203 (1999).
- <sup>2</sup>A. F. Berkowitz and K. Takano, *J. Magn. Magn. Mater.* **200**, 552 (1999).
- <sup>3</sup>M. Finazzi, L. Duò, and F. Ciccacci, *Surf. Sci. Rep.* **62**, 337 (2007).
- <sup>4</sup>H. Ohldag, T. J. Regan, J. Stöhr, A. Scholl, F. Nolting, J. Lüning, C. Stamm, S. Anders, and R. L. White, *Phys. Rev. Lett.* **87**, 247201 (2001).
- <sup>5</sup>R. Abrudan, J. Miguel, M. Bernien, C. Tieg, M. Piantek, J. Kirschner, and W. Kuch, *Phys. Rev. B* **77**, 014411 (2008).
- <sup>6</sup>R. de Masi, D. Reinicke, F. Müller, P. Steiner, and S. Hüfner, *Surf. Sci.* **515**, 523 (2002).
- <sup>7</sup>P. Luches, M. Liberati, and S. Valeri, *Surf. Sci.* **532-535**, 409 (2003).
- <sup>8</sup>P. Luches, S. Benedetti, A. di Bona, and S. Valeri, *Phys. Rev. B* **81**, 054431 (2010).
- <sup>9</sup>T. J. Regan, H. Ohldag, C. Stamm, F. Nolting, J. Lüning, J. Stöhr, R. L. White, *Phys. Rev. B* **64**, 214422 (2001).
- <sup>10</sup>P. Luches, V. Bellini, S. Colonna, L. Di Giustino, F. Manghi, S. Valeri, and F. Boscherini, *Phys. Rev. Lett.* **96**, 106106 (2006).
- <sup>11</sup>S. Benedetti, P. Luches, M. Liberati, and S. Valeri, *Surf. Sci.* **572**, L348 (2004).
- <sup>12</sup>P. Luches, S. Benedetti, A. di Bona, and S. Valeri, *Nucl. Instr. Meth. B* **268**, 361 (2010).
- <sup>13</sup>V. Bellini, L. Di Giustino, F. Manghi, *Phys. Rev. B* **76**, 214432 (2007).
- <sup>14</sup>E. Gerdau, R. Rüffer, H. Winkler, W. Tolksdorf, C. P. Klages, and J. P. Hannon, *Phys. Rev. Lett.* **54**, 835 (1985).
- <sup>15</sup>R. Röhlberger, H. Thomas, K. Schlage, E. Burkel, O. Leupold, and R. Rüffer, *Phys. Rev. Lett.* **89**, 237201 (2002).
- <sup>16</sup>W. A. A. Macedo, B. Sahoo, V. Kuncser, J. Eisenmenger, I. Felner, J. Nogués, Kai Liu, W. Keune, and Ivan K. Schuller, *Phys. Rev. B* **70**, 224414 (2004).
- <sup>17</sup>W. A. A. Macedo, B. Sahoo, J. Eisenmenger, M. D. Martins, W. Keune, V. Kuncser, R. Röhlberger, O. Leupold, R. Rüffer, J. Nogués, Kai Liu, K. Schlage, and Ivan K. Schuller, *Phys. Rev. B* **78**, 224401 (2008).
- <sup>18</sup>S. Couet, K. Schlage, R. Rüffer, S. Stankov, Th. Diederich, B. Laenens, and R. Röhlberger, *Phys. Rev. Lett.* **103**, 097201 (2009).
- <sup>19</sup>B. Sahoo, W. A. A. Macedo, W. Keune, V. Kuncser, J. Eisenmenger, J. Nogués, I. K. Schuller, I. Felner, Kai Liu, and R. Röhlberger, *Hyperfine Interact.* **196**, 1371 (2006).
- <sup>20</sup>K. Schlage, R. Röhlberger, T. Klein, E. Burkel, C. Strohm, and R. Rüffer, *New Journ. Phys.* **11**, 013043 (2009).
- <sup>21</sup>S. Cottenier, V. Vanhoof, D. Torumba, V. Bellini, M. Çakmak, and M. Rots, *Hyperfine Interact.* **158**, 9 (2004).
- <sup>22</sup>R. Rüffer and A. I. Chumakov, *Hyperfine Interact.* **97-98**, 589 (1996).
- <sup>23</sup>P. Blaha, K. Schwarz, G. K. H. Madsen, D. Kvasnicka, and J. Luitz, WIEN2K, An Augmented Plane Wave + Local Orbitals Program for Calculating Crystal Properties (Karlheinz Schwarz, Techn. Universität Wien, Austria), 2001.
- <sup>24</sup>S. Blügel, H. Akai, R. Zeller, and P. H. Dederichs, *Phys. Rev. B* **35**, 3271 (1987).
- <sup>25</sup>R. Röhlberger, J. Bansmann, V. Senz, K. L. Jonas, A. Bettac, K. H. Meiwes-Broer, and O. Leupold, *Phys. Rev. B* **67**, 245412 (2003).
- <sup>26</sup>NRS program by C. L'abbe based on the CONUSS program: W. Sturhahn, *Hyperfine Interact.* **125**, 149 (2000).
- <sup>27</sup>J. G. Stevens, *Hyperfine Interact.* **13**, 221 (1983).
- <sup>28</sup>We note that the spin moment in the C layer is larger than the bulk one, 2.6 vs 2.2  $\mu_B$ ; many more Fe layers would be required to converge it to a bulk value, but due to compensation between the larger negative core and the larger positive (transferred) valence contributions, the hyperfine fields converge faster to bulk values with the number of Fe layers.
- <sup>29</sup>P. Torelli, S. Benedetti, P. Luches, L. Gragnaniello, J. Fujii, and S. Valeri, *Phys. Rev. B* **79**, 035408 (2009).